

# Elucidating the distribution of organic consolidants in wood by Neutron Tomography

Amélie NUSSER<sup>1</sup>, Stefan RÖHRS<sup>1</sup>, Andreas SCHWABE<sup>2</sup>, Sonja RADUJKOVIC<sup>3</sup>,  
Thomas BÜCHERL<sup>4</sup>, Volker DANGENDORF<sup>5</sup>, Uwe ZSCHERPEL<sup>6</sup>, Ina REICHE<sup>7</sup>,  
Kurt OSTERLOH<sup>8</sup>

<sup>1</sup> Rathgen-Forschungslabor, Staatliche Museen zu Berlin (SMB), Stiftung Preußischer  
Kulturbesitz (SPK), Berlin, Germany

<sup>2</sup> Chair of Wood and Fibre Material Technology, Technische Universität,  
Dresden, Germany

<sup>3</sup> Vorderasiatisches Museum, SMB, SPK, Berlin, Germany

<sup>4</sup> Radiochemie München RCM, Technische Universität München, Garching, Germany

<sup>5</sup> Physikalisch-Technische Bundesanstalt (PTB), Braunschweig, Germany

<sup>6</sup> Bundesanstalt für Materialforschung und –prüfung (BAM), 8.3, Berlin, Germany

<sup>7</sup> PSL University, ENSCP, Institut de recherche de Chimie Paris (IRCP) UMR 8247 CNRS  
- Centre de recherche et de restauration des musées de France, Paris, France

<sup>8</sup> retired, formerly BAM 8.3, Berlin, Germany

Contact e-mail: kurt.r.s.osterloh@gmail.com

**Abstract.** While the absorption of X-rays and gamma radiation is determined by the Z-number of the elements a specimen is composed of, it is the hydrogen making an effective contrast with neutron imaging. As a consequence, interrogating with neutrons presents a suitable tool to study the distribution of organic consolidants in materials such as wood as encountered in impregnated wooden artworks.

Four different examples of objects are presented here to demonstrate the potential of neutron CT: 1) small wooden pieces of ship wrecks (< 2 cm thickness) interrogated with cold neutrons (0.5 meV at the ANTARES facility of the FRM II in Garching) to demonstrate the potential and the limitation of using low energy neutrons, 2) a wooden statue soaked with carbolineum (fission neutrons 1.8 MeV at the NECTAR facility of the FRM II), 3) a smaller wooden figure of a skull heavily soaked with carbolineum so it was too tight for the fission neutrons used before with accelerator neutrons (broad range about 5.5 MeV at the PTB in Braunschweig) and 4) pieces of charred wood to study the impregnation with a consolidant (NECTAR, FRM II). With the exception of the last example, all results have been combined with X-ray tomography (BAM 8.3 in Berlin). In the case of the charred wood specimens (example 4) the density histograms of the neutron tomography results were compared with those obtained from untreated references. The observed gain in specific density of the soaked specimens corresponded with an increase of specific weight. All results obtained so far showed distinct distribution patterns attributable to structural peculiarities or organic consolidants providing valuable support for subsequent restoration works.



## Introduction

It is a well known fact that hydrogen containing materials are moderating neutron beams raising the problem of the achievable penetration thickness through wooden layers, i.e. the size of specimens that could be interrogated with certain energies of neutron beams. This question has been tackled earlier [1] with the result that cold neutrons are capable to penetrate layers of very few cm, higher energies are necessary for thicker layers as encountered in larger objects. As a consequence, three different neutron radiologic instruments have been used for this study that had neutron beams of various energies from a few meV to several MeV. Since the spatial distribution of the consolidants is of interest, an equipment for computed tomography (CT) was essential.

Due to the fact that wood already is a heterogeneous matrix by itself it is necessary to have some sort of reference or at least a further indication that allows to attribute certain patterns to a distribution of a soaked substance. Ideally, this would be an investigation of the specimen before and after treatment. However, this is usually impossible when interrogating cultural artefact since they have been already treated before in most cases, very often ill documented. The way to identify alternative reference information will be discussed here.

### 1. Objects and Rationale

This study focusses on wooden objects of the cultural heritage in archaeology and sacral arts. They are unique and with an unknown original state in most cases, but very often in need of conservation measures. Various organic consolidants have been and are used for this purpose to prevent decaying caused by pests, mould and environmental conditions, in some cases the deformation due to dehydration as shown in the first example in Fig. 1. It displays a wooden specimen from a sunken ship wreck [2] that was kindly provided by the Schiffmuseum in Bremerhaven, Germany. In the course of desiccation it has changed its shape. Based on its small size it was a suitable example to study the interior by interrogating with cold neutrons ( $\sim 5$  meV) that show fairly good spatial resolution in imaging. With higher energies in the MeV range, images generated with neutrons are of inferior resolution than those with X-rays, but show different specific material absorptions, i.e. reveal certain material properties. The radiographic interrogations with X-rays alone may fail show material properties indicating faint traces of a previous treatment, if at all.



**Fig. 1.** Wooden specimen from a sunken ship wreck.  
Curved shape deformation as a result of dehydration.

A century ago, the problem of biological destruction of wood was fought with organic substances such as carbolineum that was successfully applied to fences and railway sleepers, unfortunately also to wooden artefacts without considering long time effects. Such an example is shown in Fig. 2. The sculpture “Tugend der Hoffnung” (“Virtue of Hope”) to the left and the skull model to the right were taken from the baroque epitaph Reyer (1704) at the St. Laurentius church in Tönning (Schleswig-Holstein, Germany). The impregnating agent that has been used a century ago has chemically been identified as

carbolineum, a mixture of coal tar oil components classified as carcinogenic and harmful to the environment. What an image cannot express is the scent emanating from such an object. A putative protocol to revert this measure has yet to be found but this needs some profound knowledge about the interior of the objects that only can be available by tomographic methods. Interrogating objects in this size require neutrons of higher energies.



**Fig. 2.** Wooden artefacts treated with the consolidant carbolineum. The sculpture “Virtue of Hope” (left) and the sculpture of a skull (right) were taken from an epitaph.

The other problem encountered particularly with archaeological objects are damages caused e.g. by fire and heat as happened to the torso shown in Fig. 3. It was found in the ruins of Uruk in Mesopotamia and served obviously as a cultural statue in Seleucidian times around 300 BC. Owing to the damage, such specimens are rather fragile so it is impossible to transport them over a longer distance. In order to develop an effective protocol for appropriate conservation measures, studies have been performed with charred wooden pieces that have been treated with several consolidants as a replacement (mock-ups) [3]. Examples of typical substances with different uptake and distribution characteristics, linseed oil and polyvinyl butyral, (PVB) are shown in Fig. 3. It should be reminded that this study was focussed on material compositions inside of an object rather than detecting fine structured flaws.



**Fig. 3.** Heat damaged torso that was not transportable and mock-ups for testing conservation protocols. The treated specimens (bottom) and the untreated controls (top) were imaged together. The treatment consisted out of soaking with boiled linseed oil (centre) or polyvinyl butyral (PVB, right).

In the course of further conservative measures it is essential to obtain a clue to the current status of the interior of the objects to be treated and, in some cases, about the intermediate stages of a treatment. Since the consolidants used here are organic substances that are distributed in an organic matrix, it might be difficult to detect heterogeneous

distribution patterns by X-ray radiography due to the expectingly low contrast. In difference to X-rays, neutrons are efficiently absorbed by hydrogen containing materials so their radiological use promises to detect distribution patterns of organic substances in an organic matrix much more effectively. In order to achieve additional information allowing a clue about the material composition, an X-ray-CT has been produced in addition that also resolves fine structures more in detail. Only in case of using mock-ups to study the effect of various consolidants on damaged objects as shown in Fig. 3 it was possible to compare treated specimens with untreated ones. As a consequence, results from original artefacts are being presented as overlays of neutron- and X-ray-CT images and those obtained from mock-ups by showing areas of increased densities following a treatment as compared to untreated controls.

## 2. Instruments and Methods

### 2.1 Facilities

The facilities used in this study have been described previously [2-6]. In brief, the study using cold neutrons (~5 meV) was conducted at the ANTARES instrument of the FRM II neutron source in Garching, Germany [4]. At the same site, the NECTAR instrument [5] was the source of fission neutrons (1.8 MeV average energy). Since both instruments showed a parallel beam geometry, it was sufficient to scan 180° only in 1° steps. Neutrons of still higher energies in the range of 4 – 10 MeV were available at the Physikalisch-Technische Bundesanstalt (PTB) in Braunschweig. Unfortunately, this unique source, where also energy resolved neutron radiography for element sensitive imaging was feasible, has been closed in the meantime. Normally, neutron CT scans were completed within 12 h. X-ray CT scans were conducted at BAM in Berlin, Germany, with a Comet X-ray tube set to 160 kV and 4 mA. The images were recoded with a Perkin-Elmer matrix detector (2048 x 2048 pixels of 200 µm x 200 µm size) and 1000 projections per scan at 15 s per frame.

### 2.2 Data processing

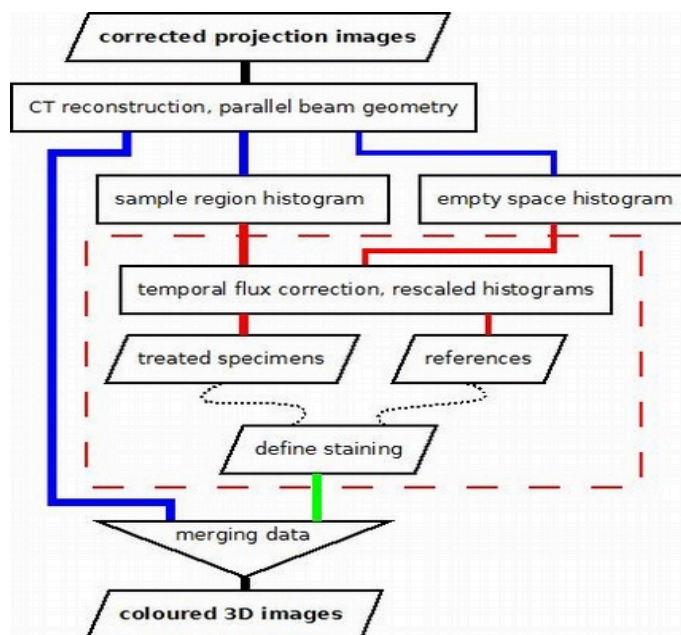


**Fig. 4.** Flow chart showing the data processing to show areas of increased density following a treatment. Coloured lined tracks: spatial 3D image data (blue), histogram data (red) and staining selection (green).

The raw images obtained from the neutron radiographic instruments were strewn with dotted interferences so they had to be filtered accordingly. This has been achieved with algorithms specially developed for this purpose [7, 8] before starting a 3D-reconstruction. Either standard software (Octopus or VGStudio MAX 2.2 and its supplement for tomography) or own software using the slice theorem have been used for the CT reconstructions. The overlay of sections from both, the X-ray-CT and the neutron-CT needed reorientations of the 3D-images as well as a brightness, contrast and  $\gamma$  adaption across the whole 3D-imaging spaces since they were obtained from different facilities with their own properties and individual positioning of the specimens in each instrument. This was achieved with own programs written on a standard Windows 7 PC using a Lazarus-Pascal-Compiler [9]. The resulting images consist of overlays of cuts through both, the neutron (blue or green) and the X-ray (red) data sets after adjusting the neutron data to align with those from the X-ray reconstructions.

The steps of how to compare treated specimens with untreated controls in a mock-up study are listed in a flow chart shown in Fig. 4. Starting with the spatial reconstruction the image data are kept for subsequent staining of areas showing increased densities (blue line on the left). Partial volumes representing the body of the specimen and an empty space were selected for calculating histograms (red lines). The latter ones were used for correcting for intensity fluctuations from one CT scan to another one (90% limit as a “white” offset). By this way, all histograms have been adjusted to a common scale. Based on the histograms of the treated and the untreated specimens, the ranges of grey values representing the density gains due to the uptake of the consolidants as well as overlaps between both groups are assigned to colours ranging from blue to red. All processes in the dashed red box in the flow chart were completed within an ordinary spreadsheet program. The last step of merging the colour coding with the spatial image data was completed with another special own program [9]. As a tool for spatial presentation, the public domain program ImageJ has been used with the 3D viewer plug-in [10].

### 3. Results and Discussion

#### 3.1 An example of small objects in a cold neutron beam

The specimen shown in Fig. 1 has successfully been interrogated both with cold neutrons and with X-rays. The combined result of both technologies can be seen in Fig. 5 as an overlay of cross sections at the same location where the neutron image is displayed in blue while the X-ray one is stained in red. It is rather obvious that more hydrogen material is located close to the surface indicating putative traces of previous interventions. However, any further interpretation in this direction requires chemical confirmation. At least, this result indicates the sites where to probe for samples in a future dedicated study.

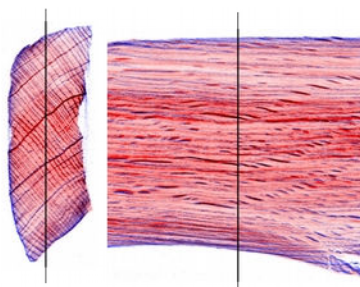


**Fig. 5.** Overlay of cross section images taken from neutron and X-ray CT of the specimen shown in Fig. 1. Blue colour: neutron-CT, red colour: X-ray-CT, left: cross section, right longitudinal section.

### 3.2 Interrogation with high energy neutrons

The sculpture shown in Fig. 2 was interrogated with neutrons at the NECTAR instrument and with X-rays at BAM. The result is shown in Fig. 6 as overlays of cuts through the CT data of the respective technologies with the green colour for the neutron technology and the red colour for the X-ray absorption. The neck region and areas close to the surface with many worm holes contained more organic material than the core region. The horizontal nail on the left side was only seen in the X-ray image and penetrated by neutrons. Very obviously the head was replaced in one of the previous conservation campaigns that explains the flawless appearance of the face as it can be seen in Fig. 2. However, there is nothing mentioned in the conservation documents, only a suggestion in this direction.

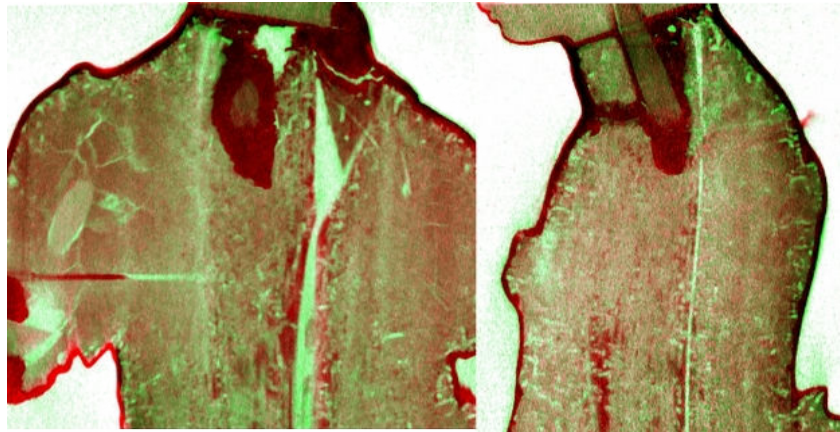


**Fig. 6.** Overlay of longitudinal cross sections of the sculpture shown in Fig. 2 on the left. The images were produced in the same manner as in Fig. 5, green: neutron-CT, red: X-ray-CT.

The model of the skull shown to the right in Fig. 2 was heavily soaked with carbolineum that could have been realised by the scent emanating. As a consequence, an attempt to interrogate this object at the NECTAR instrument remained without any success, neutrons of higher energy were requested. At that time, they were available at the PTB, and a neutron CT was successfully performed at that site. The result is shown in Fig. 7 in a spatial overlay of both CT results, red for the X-rays and green for the neutrons. The green of the hydrogen content is visible even through then red coating in the surface rendering presentation. While the coating obviously consisted of materials that absorb predominantly X-rays the whole inner space was prevailed by organic substances with minor variation in concentration. Obviously, the worm holes are filled with carbolineum.

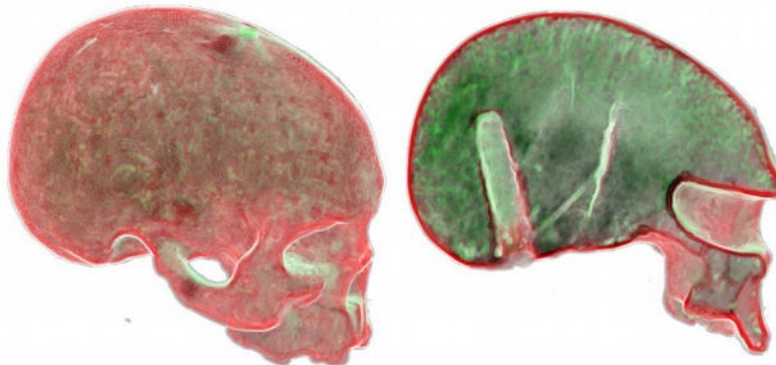


**Fig. 7.** X-ray CT (red) and neutron CT (green) overlay of the specimen to be seen in Fig. 2 on the right. The carbolineum impregnation is visible both, in the translucent surface rendering (left) and in the cut (right).

### 3.3 Correlating an uptake of consolidants with the spatial density distribution

It appears to be a recommendable practice to study preservation protocols with mock-ups rather than applying them directly to delicate original objects. The overall density of the interrogated specimens were easily determined by their weight and the volume calculated from the CT results. Generally, an increase in density was correlated with a shift towards higher values in the related histograms as expected, but not always quantitatively as demonstrated in Fig. 8 with the two consolidants linseed oil and PVB. In the first case, the density gain was 28% while it was 4% only in the latter one.

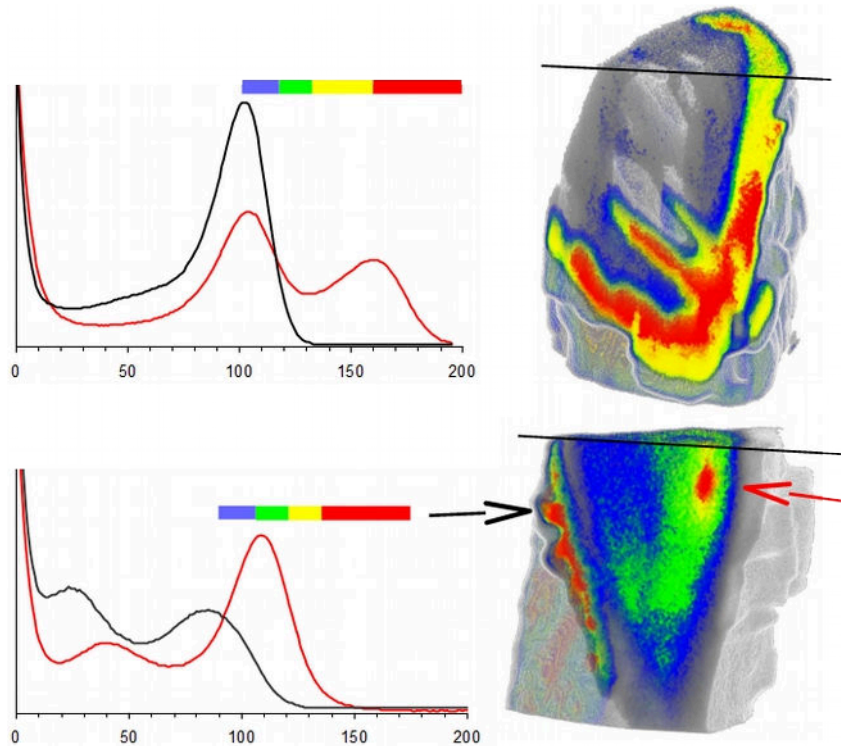


**Fig. 8.** Shifted density distributions in histograms and regions of increased densities in lateral cuts. Histograms with colour coding (left) and lateral cuts (right), treatment: linseed oil (top) and PVB (bottom), red line in histograms (frequency vs. grey values bright to dark): with treatment, black line: untreated control.

In case of the treatment with linseed oil, the density shift following a treatment seen in the related histogram is in good agreement with the expansion of areas with increased densities exceeding those of the control (yellow and red) with low areas of overlaps (blue and green). A different situation is encountered with the PVB where the density shift was less pronounced than in the previous example. However, it was larger than it could have been expected from the measured density increase of 4% only. A plausible explanation has been found in the distribution pattern shown in the lateral cut on the lower right within Fig. 8. Actually, two different sites of increased densities have been identified with distinctive characteristics related to their surrounding. One of them is located within the char close to the surface (black arrow), the other one within the bulk of the interior but with large adjacent areas of overlaps coded by the blue and green colour. As a consequence, only the increase detectable at the first site could be attributed to the treatment while the other one merely might be the result of structural differences between the treated specimen and the control not detectable at the beginning of the experiment. The red spot marked with the red arrow in Fig. 8 was attributable to a knot while nothing in this direction could be seen in the control. This example demonstrates the importance of an adequate interpretation of both together, numerical analytical results and images.

## 4. Conclusion

The combination of neutron and X-ray tomography revealed features of the interior of the objects interrogated that were not detectable from the surface. While the fine structures were resolved by X-rays clues on the material composition can be derived from the neutron CT. Finally, the overlay to the results from both technologies allow a more complex insight into the interior of the interrogated object that might provide valuable information to project future conservative measures. Analysing the density profiles of the neutron CT with subsequent spatial colour tagging the areas characterised by certain density ranges help to identify probing sites for further chemical analysis. Having both, numerical results and images together provides more information than each one by itself.

## Acknowledgements

This project was supported by the Deutsche Bundesstiftung Umwelt (DBU) under the grant Az. 30165 – 45 and by the Berliner Antike-Kolleg (BAK-TT8-2015). The valuable help received from several colleagues is gratefully acknowledged, namely from S. Söllradl at the NECTAR instrument, B. Redmer, S. Hohendorf and C. Bellon for achieving the X-ray tomography results and from M. Freitag, N. Wrobel, S. Simon, M. Hilgert and U. Ewert for many fruitful discussions. The charred wood specimens were kindly provided by the Harzköhlerei Stemberghaus in Hasselfelde, Germany.

## References

- [1] K. Osterloh, D. Fratzscher, M. Jechow, T. Bücherl, B. Schillinger, A. Hasenstab, U. Zscherpel, U. Ewert (2011): Limited View Tomography of Wood with Fast and Thermal Neutrons, DIR 2011 International Symposium on Digital Industrial Radiology and Computed Tomography, 20-22 June 2011, Berlin, Germany, P14, <https://www.ndt.net/article/dir2011/papers/p14.pdf>,
- [2] K. Osterloh, D. Fratzscher, A. Schwabe, B. Schillinger, U. Zscherpel, U. Ewert (2011): Radiography and partial tomography of wood with thermal neutrons, Nucl. Instr. & Meth. in Physics Res. (NIM) A 651, pp. 236-239,
- [3] K. Osterloh, A. Nusser, S. Röhrs, S. Radujkovic, A. Schwabe, S. Söllradl, I. Reiche (2015): Verteilungsstudien von Festigungsmitteln in verkohlten Objekten mittels der Neutronen-Computertomographie, 8. N.i.Ke.-Workshop, 2015, N.i.Ke. Schriftenreihe des Netzwerks zur interdisziplinären Kulturguterhaltung in Deutschland, ISSN 2567-1251, 94-99,
- [4] M. Schulz, B. Schillinger: Heinz Maier-Leibnitz Zentrum et al. (2015). ANTARES: Cold neutron radiography and tomography facility. Journal of large-scale research facilities, 1, A17. <http://dx.doi.org/10.17815/jlsrf-1-42>,
- [5] T. Bücherl, S. Söllradl: Heinz Maier-Leibnitz Zentrum et al. (2015). NECTAR: Radiography and tomography station using fission neutrons. Journal of large-scale research facilities, 1, A19. <http://dx.doi.org/10.17815/jlsrf-1-45>,
- [6] A. Nusser, M. Freitag, A. Fuhrmann, C. Herm, K. Osterloh, I. Reiche, A. Schwabe, S. Simon (2015): Analyse historischer Carbolineumimprägnierungen als Grundlage konservatorischer Dekontaminierung und modellhafte Erprobung neuer Sanierungstechnologien, Abschlussbericht zum Projekt, gefördert unter Az 30165 von der Deutschen Bundesstiftung Umwelt, Berlin, 2015, Hornemann Institut, HAWK Hochschule für angewandte Wissenschaft und Kunst, Hildesheim/Holzminden/Göttingen, [https://www.hornemann-institut.de/german/epubl\\_projekte149.php](https://www.hornemann-institut.de/german/epubl_projekte149.php),
- [7] K. Osterloh, T. Bücherl, Ch. Lierse von Gostomski, U. Zscherpel, U. Ewert, S. Bock (2011): Filtering algorithm for dotted interferences, Nucl. Instr. and Meth. in Physics Res. A 651, 171-174,
- [8] K. Osterloh, T. Bücherl, U. Zscherpel and U. Ewert (2012): Image recovery by removing stochastic artefacts identified as local asymmetries, Journal of Instrumentation 7 C04018, <http://iopscience.iop.org/1748-0221/7/04/C04018>,
- [9] Free Pascal Lazarus Project, version 1.6 (2016), <http://www.lazarus-ide.org/>
- [10] K.U. Barthel (2014): Volume Viewer, <https://imagej.nih.gov/ij/plugins/volume-viewer.html>, W. Rasband: ImageJ 1.48v (2012), <https://imagej.nih.gov/ij/>.